Heliyon 10 (2024) e27715

Contents lists available at ScienceDirect

Heliyon

journal homepage: www.cell.com/heliyon

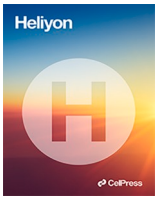

Research article

Innovative ionic liquid pretreatment followed by wet disk milling treatment provides enhanced properties of sugar palm nano-fibrillated cellulose

A.S. Norfarhana [a,b], R.A. Ilyas [a,c,d,e,*], Norzita Ngadi [a], Mohd Hafiz Dzarfan Othman [a,f]

[a] Department of Chemical Engineering, Faculty of Chemical and Energy Engineering, Universiti Teknologi Malaysia, 81310 UTM Skudai, Johor, Malaysia
[b] Department of Petrochemical Engineering, Politeknik Tun Syed Nasir Syed Ismail, Pagoh Education Hub, 84600 Pagoh Muar Johor, Malaysia
[c] Centre for Advanced Composite Materials (CACM), Universiti Teknologi Malaysia (UTM), Johor Bahru 81310, Johor, Malaysia
[d] Institute of Tropical Forestry and Forest Products (INTROP), Universiti Putra Malaysia, Serdang 43400, Selangor, Malaysia
[e] Centre of Excellence for Biomass Utilization, Universiti Malaysia Perlis, 02600, Arau, Perlis, Malaysia
[f] Advanced Membrane Technology Research Centre (AMTEC), Faculty of Chemical and Energy Engineering, Universiti Teknologi Malaysia, 81310 Johor Bahru, Johor, Malaysia

ARTICLE INFO

Keywords:
Sugar palm fiber
Ionic liquid pretreatment
Isolation
Wet disk mill
Cellulose nanofiber

ABSTRACT

In order to accommodate the increased demand for innovative materials, intensive research has focused on natural resources. In pursuit of advanced substances that exhibit functionality, sustainability, recyclability, and cost-effectiveness, the present work attempted an alternative study on cellulose nanofibers derived from sugar palm fiber. Leveraging an innovative approach involving ionic liquid (IL) pre-treatment, bleaching, and wet disc mill technique, nano-fibrillated cellulose (NFC) was successfully obtained from the sugar palm fiber source. Remarkably, 96.89% of nanofibers were extracted from the sugar palm fiber, demonstrating the process's efficacy and scalability. Further investigation revealed that the sugar palm nano-fibrillated cellulose (SPNFC) exhibited a surface area of 3.46 m^2/g, indicating a significant interface for enhanced functionality. Additionally, the analysis unveiled an average pore size of 4.47 nm, affirming its suitability for various applications that necessitate precise filtration. Moreover, the surface charge densities of SPNFC were found to be −32.1 mV, offering opportunities for surface modification and enhanced interactions with various materials. The SPNFC exhibit remarkable thermal stability, enduring temperatures of up to 360.5 °C. Additionally, the isolation process is evident in a significant rise in the crystallinity index, escalating from 50.97% in raw fibers to 61.62% in SPNFC. These findings shed light on the vast potential and distinct features of SPNFC, opening the path for its application in a wide array of industries, including but not limited to advanced materials, biomedicine, and environmental engineering.

* Corresponding author. Department of Chemistry, Faculty of Chemical and Energy Engineering, Universiti Teknologi Malaysia, 81310 UTM Skudai, Johor, Malaysia.
E-mail address: ahmadilyas@utm.my (R.A. Ilyas).

https://doi.org/10.1016/j.heliyon.2024.e27715
Received 10 December 2023; Received in revised form 5 March 2024; Accepted 5 March 2024
Available online 7 March 2024
2405-8440/© 2024 The Authors. Published by Elsevier Ltd. This is an open access article under the CC BY-NC-ND license (http://creativecommons.org/licenses/by-nc-nd/4.0/).

1. Introduction

The research of green and environmentally benign materials has been increasingly important in recent generations since there is a growing worldwide concern for conserving resources, reducing pollution, and adopting eco-conscious industrial practices. Interestingly, recent research explores using agricultural waste as a cost-effective alternative to commercial inorganic materials in advanced materials applications [1–3]. Embracing the concept of a circular economy, this waste can be converted into bioenergy, biofuel, biogas, and bicomposite products, contributing to diverse industries and addressing environmental challenges [4,5]. Leveraging the valuable content of agricultural waste offers advantages like cost-effectiveness, renewable resources, and source diversity [6,7]. Cellulose, a ubiquitous biopolymer found in the cell walls of various plants, including agricultural waste has been increasingly recognized for its transformative potential in the world of materials science [8]. Innovative cellulose paper composites made from agricultural waste (jackfruit peduncles) were synthesized for heat management applications in biomedical electronics by Devarajan et al. [9].

Nanocellulose (NC) is a cellulosic substance that can be extracted from agricultural waste and has nanoscale dimensions [10]. NC represents a flexible and easily accessible nanomaterial because of its high hydrophilicity, large surface area, outstanding aspect ratio, excellent strength, and stability [11]. Cellulose nanofibrils (CNF), cellulose nanocrystals (CNC), and bacterial nanocellulose (BC) are the three main types of nanocellulose materials that are classified based on the extraction methods used. CNF and CNC employ top-down processing methods [12], while BC originates from bacteria, synthesizing nanofibers from the bottom up [13,14]. Rajan et al. [15] fabricated CNF from red banana empty fruit bunches using chemical and ball milling techniques for lightweight structural applications, achieving improved web structure porosity and widths (50–75 nm) through surface modification. Raghav et al. [16] efficiently isolated CNC from used paper egg carton boxes through sequential organosolv and cyanamide-activated hydrogen peroxide treatments, citric acid hydrolysis, and in-situ generation. The resulting CNC exhibit a rod-like structure with uniformly dispersed AgNPs, showcasing the potential of the bio-nanocomposite film for active packaging applications. D'orame-Miranda et al. [17] produced BC using *Gluconacetobacter entanii*, yielding 2.816 $\pm$ 0.040 g/L of cellulose in 28 days which encouraged the production of biocomposites.

Among NC, CNF have emerged as a groundbreaking class of materials due to their exceptional properties and versatility [18]. The unique properties of CNF, such as their high surface area, remarkable mechanical strength, and biodegradability, have propelled research into their utilization in diverse fields ranging from advanced materials to environmental remediation [19,20]. Multiple techniques have been explored for the pretreatment of agricultural waste for nanocellulose extraction. Current pretreatment method for lignocelluloses mainly relies on the use of harsh chemicals, which are difficult to recycle and not environmentally friendly [21]. Research has been developed to propose a greener approach to pretreat the lignocellulose. Intriguingly, some study revealed that ionic liquid (IL) pre-treatment offers a compelling alternative to conventional cellulose extraction methods. The use of IL, and more specifically 1-butyl-3-methylimidazolium chloride ([Bmim][Cl]), was shown to be successful in cellulose fractionation by Mohtar et al. [22], which achieved 52.72% wt. This is attributed to its superior capacity to disintegrate cellulose in a more efficient and environmentally sustainable manner [23]. This approach is crucial to obtain high-quality of nanocellulose for various applications. The application of IL pre-treatment serves to dissolve and deconstruct the cellulose within lignocellulosic biomass, rendering it more manageable [24]. IL effectively eliminate the amorphous cellulose, hemicellulose, and lignin from the cellulose structure, thereby yielding nanocellulose of exceptional quality [25]. Using IL as a pretreatment technique greatly improves the processing performance of cellulose-rich fibers for biocomposite manufacture, as demonstrated by numerous investigations [26,27]. IL-treated cellulose fibers have better crystallinity and thermal stability than untreated wood, according to a study by Moniruzzaman and Ono [28]. Additionally, Ullah et al. [29] employed IL technology to isolate silica from rice husk, which offers a distinctive benefit in terms of energy conservation due to the absence of thermal energy consumption.

Bleaching treatment is integral to the extraction process of nanocellulose from agricultural waste as it serves to enhance purity and remove impurities from the fibers [30,31]. By eliminating components such as lignin, hemicellulose, and non-cellulosic materials, bleaching ensures that the resulting nanocellulose possesses a higher degree of purity, crucial for its intended applications [32]. Utilizing oxygen-based bleaching agents like hydrogen peroxide (H_2O_2) aligns with principles of green chemistry, offering eco-friendly alternatives that effectively remove impurities without introducing harmful residues [33]. Besides, this preference for eco-friendly practices over hazardous sodium hypochlorite (NaClO) and sodium chlorite ($NaClO_2$) underscores a commitment to sustainable nanocellulose extraction practices [34]. The resulting nanocellulose, characterized by enhanced purity and preparedness for various applications, underscores its versatility in fields such as biomedical devices, packaging, and advanced composite materials [33,35]. Rizwan et al. [36]explored the efficiency of various bleaching reagents in isolating and characterizing cellulose from *Alstonia scholaris*. Their findings revealed that H_2O_2 exhibited superior efficiency compared to NaClO and $NaClO_2$ in cellulose extraction. Thus, the strong oxidizing properties of H_2O_2 contribute to breaking down complex structures, preparing the fibers for subsequent mechanical treatments.

The CNF is primarily produced using a mechanical disintegration process that employs a mix of impact and shear forces, resulting in particles with both crystalline and amorphous portions [37]. In a top-down treatment procedure, a robust mechanical shearing technique enables the gradual breakdown of constituent microfibrils, thus rendering it easier to produce cellulose nanofibrils Cellulose nanofibrils (CNF) from cellulose pulp fibers [38]. Mechanical extraction, which involves refining, microfluidization, milling, grinding, cryo-crushing, and ultrasonication, produces lengthy chains of microfibrils and nanofibrils [39] Fibril-like structures with diameters less than 100 nm and lengths in the micrometer scale tend to appear in CNF developed via mechanical procedures. Interestingly, wet disk mill (WDM) is increasingly favored for its remarkable energy efficiency compared to other milling techniques, effectively breaking down cellulose into nanofibrils and yielding CNF with exceptional surface properties and distinctive characteristics [40]. Yasim-Anuar et al. [41] successfully extracted cellulose nanofibrils (CNF) from waste paper by the WDM method. Their findings reveal that this

green approach effectively reduced the size of wastepaper fibers from micrometer scale to 20–40 nm after 10 milling cycles. Additionally, the CNF enhanced the tensile strength and Young's modulus of poly(R)-3-hydroxybutyrate-*co*-(R)-3-hydroxyhexanoate (PHBHHx) by 19% and 12%, respectively, compared to the neat polymer.

Sugar palm fiber (SPF) scientifically known as *Arenga pinnata* is one of the plentiful natural fibres found in Malaysia, however it has not been widely employed as well [42]. Among the various sources of nanocellulose, SPF extracted from sugar palm tree, has garnered particular interest as an abundant and renewable raw material that can be harnessed to produce CNF [43]. SPF exhibits unique properties, making it a valuable resource for a range of applications including automotive [44,45], construction [46], and packaging [47–49]. NC derived from SPF has been extensively utilized as a reinforcing agent in polymer composites owing to its abundant supply and exceptional mechanical properties [50,51]. In addition, SPF possesses the benefit of serving as a prospective reservoir of cellulose derived from its bunch, trunk, and frond [52]. Notably, it possesses high biodegradability, aligning with environmental sustainability goals as it naturally decomposes, leaving a minimal ecological footprint [46]. This cellulose often has a fibrillated structure, comprising nanofibers or microfibrils, which provides a high surface area, making it suitable for applications in nanotechnology and advanced materials [49]. Additionally, the high surface area and fine structure of sugar palm nancellulose make it suitable for water treatment and filtration applications [12,53].

The combined effects of IL pre-treatment, H_2O_2 bleaching, and WDM mechanical disintegration in the production of sugar nano-fibrillated (SPNFC) from SPF are of particular interest in this study. Notably, there is no prior record of producing nano-fibrillated cellulose from sugar palm fiber using this integrated approach. An in-depth analysis was conducted to thoroughly investigate the chemical, morphological, physical, thermal, and surface properties of the extracted SPNFC. This research employed diverse techniques, encompassing scanning electron microscopy (SEM), field electron scanning electron microscopy (FE-SEM), transmission electron microscopy (TEM), Fourier transform infrared spectroscopy (FT-IR), Brunauer–Emmett–Teller (BET), Zeta potential analyzer, X-ray diffraction (XRD), and thermogravimetric analysis (TGA). This innovative method presents a sustainable approach for developing bio-based nanomaterials with improved properties, well-suited for applications in wastewater treatment.

2. Materials and methods

2.1. Materials

Sugar palm fibres (SPF) were collected from Bahau, Negeri Sembilan Malaysia. Ionic liquid, 1-butyl-3-methylimidazolium chloride ([Bmim][Cl]) was supplied by Io-li-tech, Germany. Chemicals such as toluene (C_7H_8), ethanol (C_2H_5OH), acetone (C_2H_6O), and hydrogen peroxide (30%, H_2O_2) were purchased from Sigma-Aldrich/Merck (USA).

2.2. Ionic liquid pre-treatment and bleaching processes for SPC extraction

The process commenced by subjecting SPF to grinding and sieving procedures to achieve particles of approximately 500 μm in size. Subsequently, 10 g of finely ground SPF was packed into a thimble and underwent dewaxing utilizing a toluene/ethanol mixture (2:1, v/v) at its boiling point for a duration of 6 h in a Soxhlet extractor to eliminate pectin, wax, and other impurities. Afterward, the dewaxed SPF was rinsed with distilled water and dried in an oven at 60 °C overnight. The dewaxed SPF was mixed with ionic liquid (IL), [Bmim][Cl] and put into 250 mL round-bottom flasks at optimized conditions with a specific weight ratio of 1:3.7 (SPF/IL), heating at 124 °C for 40 min duration as followed the procedure outline by Norfarhana et al. [54]. The IL pre-treatment utilized to break down the intricate structure of sugar palm fibers without lowering its quality. Next, an equal ratio of water and acetone (1:1, v/v)

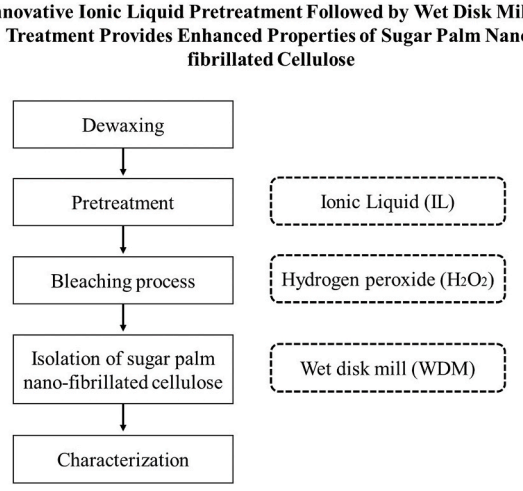

Fig. 1. Schematic illustration of SPNFC isolation.

was used to wash the mixture, and it was stirred vigorously for 30 min. The resulting suspension was filtered and washed with distilled water to get rid of any lingering IL. The residue, which was high in carbohydrates, was collected and bleached with 30% H_2O_2 for 5 h at 80 °C. According to Susi et al. [55], a bleaching process was implemented to purify the cellulose extracted from natural fibers, aiming to eliminate impurities and achieve a high level of cellulose purity. After separating the solid component from the H_2O_2 solution using vacuum filtration, the bleached sample was washed with distilled water several times to eliminate any remaining H_2O_2. This produced pure sugar palm cellulose (SPC). Lastly, the sample dried overnight at 60 °C before being securely packaged and stored at room temperature for further processing.

2.3. SPNFC extraction

Following purification, the wet disk milling (WDM) technique was employed, utilizing controlled mechanical forces in a liquid medium to fibrillate the cellulose into nano-sized fibril. Sugar palm nano-fibrillated cellulose (SPNFC) was obtained from SPC using the WDM technique as illustrated in Fig. 1. This procedure utilized a WDM high-shear ultrafine friction grinder from Grow Engineering in Adachi-ku, Tokyo, Japan. The SPC was soaked in distilled water for a duration of 72 h to facilitate the disk-milling procedure. Subsequently, approximately 2 L of fiber suspension with a concentration of 2 wt% were introduced into the grinder, subjected to 25 cycles at a rotational speed of 1800 rpm. The resulting fibers were designated as sugar palm nano-fibrillated cellulose (SPNFC). The SPNFC slurry was carefully kept in a sealed jar at 2 °C for later use. Additionally, a 10 mL sample of the slurry was freeze-dried for further characterization. This comprehensive approach, integrating the eco-friendly IL pre-treatment, peroxide bleaching, and WDM technique, was instrumental in obtaining SPNFC with distinctive properties suitable for various applications.

3. Characterization

3.1. Morphology analysis

A scanning electron microscope (Hitachi TM 3000, Japan) operating at 5 kV was employed to examine the morphology of raw SPF, IL pre-treatment, and bleaching-treated samples. The dried specimens were coated with a platinum layer between 1 and 10 nm thick before imaging. At least five SEM pictures were taken of each sample from various angles. The morphological study of SPNFC samples was performed using a Field Emission Scanning Electron Microscope (FESEM) (Hitachi SU8020, Japan) with an ultra-high resolution 1.3 nm imaging at an accelerating voltage of 1.0 kV. Advanced transmission electron microscopy (TEM) analysis was subsequently used to reveal the multidimensional nanostructure of ionized SPNFC. The Philips Tecnai 20 instrument, equipped with a 200 kV accelerator voltage and a conventional-angled sample holder, served as the primary tool for obtaining high-resolution TEM micrographs.

3.2. Fourier transform infrared (FT-IR) analysis

The aim of the infrared spectroscopy study is to figure out specific functional groups in the SPF sample under different treatment conditions. This spectroscopic examination is performed employing the Spectrum GX model instrument by PerkinElmer 2000 (USA) and analysed span from 4000 to 500 cm^{-1}, featuring a resolution of 4 cm^{-1} and a scanning speed of 20 kHz.

3.3. SPNFC yield

A 2 wt% solution of the materials was diluted with distilled water and then subjected to centrifugation at 4500 rpm for a duration of 20 min. This centrifugation process effectively segregated the nano-fibrillated material present in the supernatant, separating it from the non-fibrillated and partially fibrillated components which settled as sediments. The resultant substances were subsequently dried to a consistent weight at a temperature of 90 °C within a halogen desiccator. To determine the yield, Equation (1) was applied:

$$\text{Yield } (\%) = \left(1 - \frac{\text{weight of dried sediment}}{\text{weight of diluted sample} \times \%\ S_c}\right) \times 100 \quad (1)$$

where % Sc represents the percentage of the materials. The findings are presented as the average of data from three independent experiments.

3.4. Surface area analysis

To determine SPNFC's surface area and pore volume, a BET (Brunauer-Emmett-Teller) analysis was performed. The pore size of SPNFC was measured using a surface area and porosity analyzer (Tristar II 3020, Micromeritics, USA), which included the adsorption of nitrogen gas. The SPNFC had careful degassing by being exposed to an inert nitrogen flow [56] at 150 °C for a duration of 24 h. Subsequently, the determination of the average pore size was accomplished utilizing the bubble point technique of the Capillary Flow Porometer [57].

3.5. Zeta potential measurement

Surface charge densities of SPNFC have been evaluated via zeta potential measurements, which were conducted using the Zetasizer Nano-ZSP instrument (Malvern Instruments, Worcestershire, UK). Dynamic Light Scattering was used in this study to figure out the approximate size of SPNFC and to demonstrate the surface charge features of nanoparticles at a temperature of 25 °C.

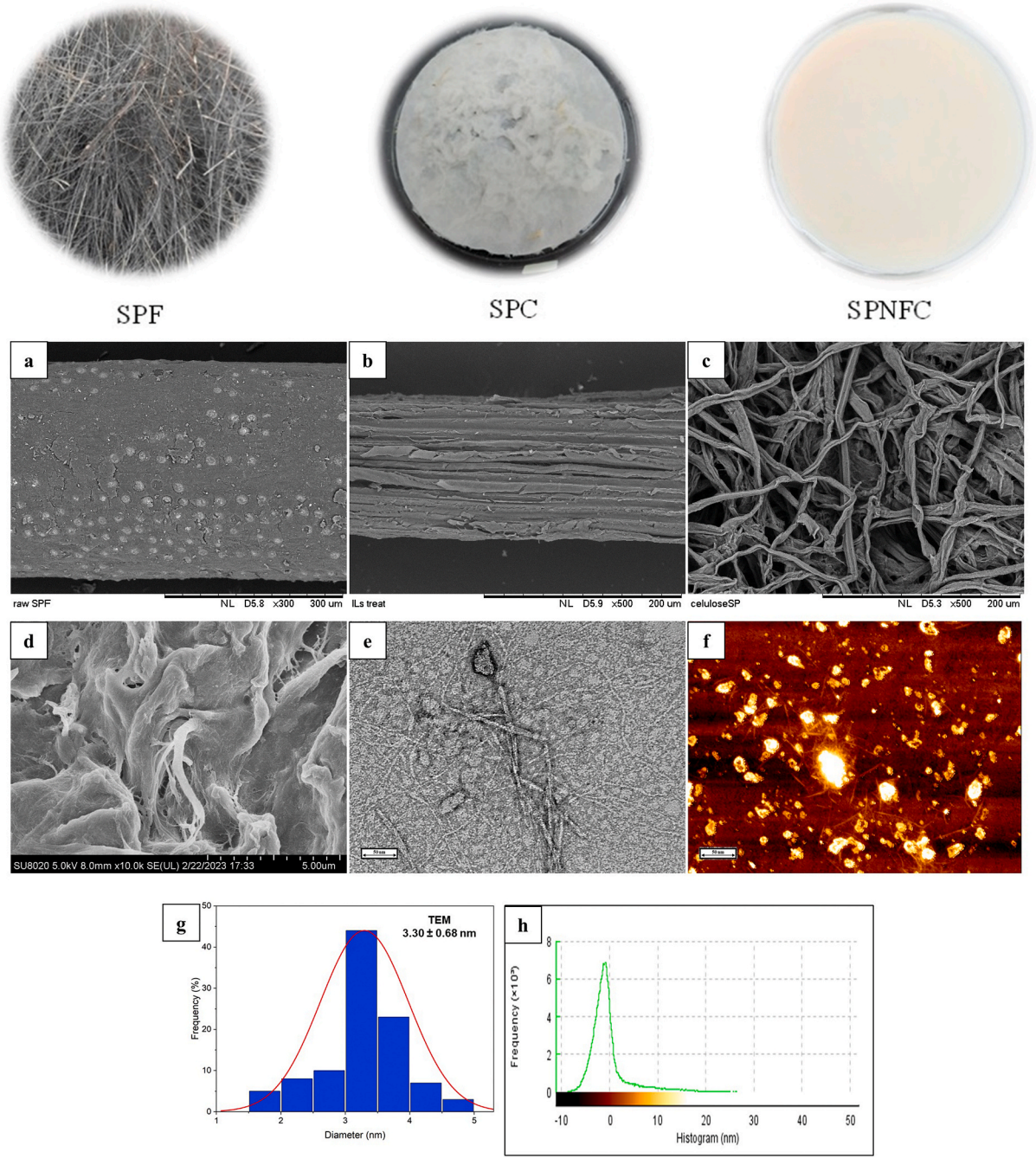

Fig. 2. Images of SPF, SPC and SPNFC, SEM images for (a) Raw SPF (b) IL treatment (c) SPC, FESEM images for (d) SPNFC, TEM image for (e) SPNFC, AFM image (f) SPNFC, TEM micrograph of length and diameter histograms of SPNFC (g), and AFM micrograph of diameter of SPNFC (h).

3.6. X-ray diffraction (XRD)

The diverse treatments' impact on the X-ray diffraction patterns of the SPF sample was investigated utilizing the Rigaku D/max 2500 X-ray powder diffractometer (Tokyo, Japan). Employing CuKα radiation (λ = 0.1541 nm) and scanning within the 2θ range of 5–40° at a speed of 2.00/min, the instrument unveiled the intricate details of the patterns. The crystallinity index (CrI%) was calculated using Equation (2), which was derived by Segal et al. [58] based on the intensity of the diffraction pattern.

$$\mathrm{CrI\%} = \frac{I_{200} - I_{am}}{I_{200}} \times 100\% \quad (2)$$

A noteworthy observation is the peak intensity maxima of I_{200}, which is located at an approximate 2θ = 22, indicating the lattice plane. and while two highest peaks of I_{am} around 2θ = 18 [59,60]. The intensity of this measurement peak was following the pattern in Segal's peak height that emerged [61].

3.7. Thermogravimetric analysis (TGA)

Thermogravimetric Analysis (TGA), delving into the intricacies of weight loss as temperature ascends, provided a thorough exploration into the thermal degradation patterns of SPF. A PerkinElmer TGA 4000 (USA) was used for evaluating the thermal stability of SPF throughout various treatments. The experimental setup involved aluminum pans within a nitrogen atmosphere, spanning temperatures from 25 °C to 800 °C and a heating rate of 10 °C/min.

4. Results and discussion

4.1. Morphological properties

Fig. 2 presents images of the raw SPF, SPC, and SPNFC. The primary differentiating factors among these fibers are their color and size. The use of IL and bleaching treatments significantly altered the color of the sugar palm fibers, while the mechanical disintegration process notably reduced their size. The figures illustrates the morphological transformations of SPF subjected to various treatments. SEM photographs of untreated SPF, SPF that has been treated with IL, and the consequent SPC samples are shown in Fig. 2(a–c). Fig. 2a depicts untreated SPF with an apparently uniform surface, despite being visibly coated with substances such as wax, pectin, lignin, and hemicellulose. As seen in Fig. 2b, after being treated with [Bmim][Cl], these encrusting components are partially removed from the exteriors of the cellulose fiber bundles. This treatment renders the fibers rougher and more porous due to the partial removal of components, including hemicellulose, lignin, wax, and impurities, along with size reduction. Thus, the lignin structure in lignocellulosic materials degrades, hence increasing the accessible surface area for future bleaching [62,63], as seen in Fig. 2c. After several processes, including bleaching, the binding substance lignin is eliminated, and the cellulose bundles separate into micro-sized fibers when their ties are dissolved [64]. After being bleached, SPF (known as SPC) was subjected to further mechanical processing in a wet disk mill (WDM), resulting in nano-fibrillated cellulose. A morphological study of SPNFC by FESEM is shown in Fig. 2d. The micrograph illustrates that the SPC, treated with WDM, displays an uneven structure that suggests nano-fibrillation. Because of the placement of mill stones prior to the WDM process, shearing and frictional forces are applied to the outermost layer of cellulose fibers, causing this occurrence. Within is particular framework, cellulose fibers undergo significant high-velocity impact forces and friction when they are crushed between opposed to grinding disks [41].

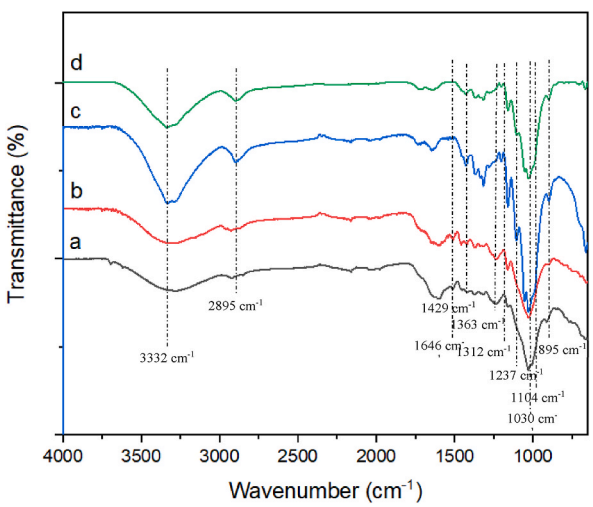

Fig. 3. FTIR spectra of (a) raw SPF (b) IL-treated SPF (c) SPC and (d) SPNFC.

To gain a better understanding of the scale on which SPNFC operates, extensive nanoscale studies were carried out using TEM. These studies as seen in Fig. 2e, SPNFC has a thread-like shape with some dimensional variation. Particularly, the WDM process yields SPNFC a diameter size of roughly 3.30 ± 0.68 nm as shown in Fig. 2g. These TEM-based findings are in line with earlier studies that have documented nanofibril widths from a variety of sources, such as *Agave gigantea* (AG) fiber (4.07 nm) [65], Nigerian grasses (3–5 nm) [66], and *Gigantochloa scortechinii* bamboo fibers (5–10 nm) [67]. Notably, the dimensions are significantly smaller than the size of an empty fruit bunch (EFB) (17.85 nm) [68] and waste paper (20–40 nm) [41]. Additionally, AFM was used as a reference technique for evaluating the morphology and size of the nanocellulose [69]. The AFM-obtained topography image of CNF reveals a thread structure, consistent with the analysis using TEM. As indicated in AFM analysis (Fig. 2f), the average size of CNF was slightly smaller than that determined by TEM analysis, as evidenced by the AFM histogram data in Fig. 2h. This observed variation in nanoparticle size is attributed to the convolution tip effect inherent to AFM measurements [49].

4.2. Functional group

Fig. 3 (a–d) represents the distinct functional group attributes of raw SPF, IL-treated SPF, SPC, and SPNFC respectively, whereas Table 1 provides a summary of the stated FTIR peak values. Spectral bands of raw SPF were seen at 3332, 2895, 1646, 1429, 1363, 1312, 1237, 1104, 1030 and 895 cm^{-1}. The notable peaks situated between 3500 cm^{-1} and 3200 cm^{-1} denote the presence of O–H groups found throughout the SPF fibers. The hydroxyl groups contained in the aliphatic and phenolic structures of cellulose, hemicellulose, and lignin are most likely responsible for this [22,70]. The absorption at 2895 cm^{-1} is due to the C–H stretching [27]. The spectral peak at 1646 cm^{-1} has been attributed to water's bending mode absorbs by cellulose as reported by The absorption observed at 2895 cm^{-1} corresponds to C–H stretching, while the spectral peak at 1646 cm^{-1} is attributed to the bending mode of water absorbed by cellulose, a phenomenon previously reported by Li et al. [71].

As reported by Lima et al. [79] the peak observed at 1237 cm^{-1}, representing the C–O stretching vibration of the acyl group in lignin, exhibited a shift following bleaching treatment. Consequently, it can be deduced that the bleaching processes effectively removed a substantial portion of the lignin and hemicellulose constituents from the SPF. After bleaching treatment, a noticeable increase in the intensity of peaks at 1429, 1363, 1312, 1159, 1104, 1052, and 1030 cm^{-1} was evident. These peaks associated with various vibrations, including C–*O*–C stretching, C–H_2 deformation, C–H_2 rocking, C–*O*–C glycoside ether, C–O pyranose ring stretching, and C–O stretching of a primary alcohol, which are characteristic of cellulose peaks in carbohydrates [80]. The recognizable band located around 895 cm^{-1} can be attributed to stretching vibrations of C–*O*–C, indicating the availability of -glycosidic bonds in cellulose [81,82].

4.3. SPNFC yield

A remarkable 65.32 wt% of cellulose was efficiently extracted from SPF through the synergistic treatments. The resulting CNF yield was notably high at 96.89 wt%, demonstrating the capable potential of the approach for scaled extracting. Table 2 elucidates the distinctive properties of the synthesized SNPC in comparison to diverse lignocellulosic biomasses. Interestingly, this study achieved a higher cellulose yield of 82 % from jack fruit peduncle [9], 45 % from red banana empty fruit bunches [15], 65–70 % from millet husk [83], 78 % from *Cuscuta reflexa* [84], 94.83 % from Sunn hemp [85], 89.39 % from *Agave gigantea* [86], 65 % from sugarcane bagasses [87], 23.54 % from rice husk [88] and 84.75 % from timoho fiber [89], respectively. This result highlights the feasibility and effectiveness of this approach as implemented on a larger scale. Employing mechanical defibrillation methods on cellulose fibers using WDM leads to the creation of nano-fibrillated cellulose (NFC), significantly boosting the SPNFC yield.

During the WDM treatment, nanofibers experience heightened exposure to wet impact and shear forces, resulting in a substantial conversion rate into nanofibers [93]. In contrast to the yield of cellulose nanofibers obtained through TEMPO-oxidation of wood fibers, this study showcases a remarkable yield, surpassing the 30.46% and 44–55% yield reported by Masruchin et al. [94] and Jonasson et al. [95], respectively. Interestingly, this study demonstrates a far higher yield of nano-fibrillated cellulose (NFC) from sugar palm fiber (SPF) compared to previous research [43,96], which generated a 29% yield of SPF nanocrystalline cellulose by a chemical method including acid hydrolysis and 92.52% of SPF nanofibrillated cellulose by a mechanical method which is high pressurized

Table 1
List of SPF-sample FTIR peaks and their associated frequencies.

Wavenumber (cm^{-1})	Structural Polymer	Peak Assignment	Ref.
3332	O–H stretching intramolecular hydrogen bond	–	[72]
2895	C–H stretching	–	[73]
1429	C–*O*–C stretching	Cellulose	[73]
1363	C_{-2}^{H} deformation vibration	Cellulose	[74]
1312	C_{-2}^{H} rocking vibration	Cellulose	[75]
1237	C–*O*–C aryl-alkyl ether	Lignin	[75]
1160	C–*O*–C glycoside ether band	Cellulose	[76]
1104	C–O pyranose ring stretching vibration	Cellulose	[76]
1052	C–*O*–C stretching ethyl vibration	Cellulose	[77]
1030	C–O stretching of primary alcohol	Cellulose and hemicellulose	[74]
895	C–O stretching	Cellulose	[78]

Table 2
Comparison of the morphological, physicochemical, and thermal of SPNFC with other common lignocellulosic fibers.

Lignocellulosic biomass	Extraction method	Morphological properties		Chemical properties	Physical properties	Thermal properties	Ref.
		Shape	Diameter (nm)	Cellulose yield (wt%)	CrI (wt%)	Temperature maximum (T_m, °C)	
Jack fruit peduncle	- Acidified chlorination - Alkalization treatment - Acid hydrolysis	Cylindirical structure	27300	82.00	79.5	349	[9]
Red banana empty fruit bunches	- Alkaline treatment - $NaClO_2$ bleaching - Ball mill treatment	Web-like structure	15–35	45.00	69.5	421	[15]
Millet husk	- Alkaline treatment - ($NaOH + H_2O_2$) bleaching - Steam explosion - Acid hydrolisis + homogenization treatment	Web-like arrangement	10–12	65–70	58.45	341	[83]
Cuscuta reflexa	- Alkaline treatment - Steam explosion treatment	Thread network structure	10–30	78	67	363	[84]
Sunn hemp	- Alkaline treatment - DMSO treatment - Acid hydrolysis treatment	Web-like structure	55 ± 13	94.83	72.52		[85]
Agave gigantea	- Alkaline treatment - ($NaOH + CH_3COOH +$ NaClO2) bleaching - Ultragrinding + ultrasonication treatment	Fibril-fibril structure	4.07	89.39	65.21	355.91	[86]
Sugarcane bagasse	- Alkaline treatment - Acid treatment - Alkaline treatment - High speed grinding	Spherical/rod like structure	57.07	65.00	58.32	–	[87]
Rice husk	- Alkaline treatment - H_2O_2 bleaching - HPH treatment	Fiber networks	10.15–12.42	23.54	62–72	>380	[88]
Timoho fiber	- NaClO2 bleaching - Alkaline treatment - Acid hydrolysis	Glycosidic network	68.94 ± 8.36	84.75	71.14	365.36	[89]
Wheat straw	- ($CH_3COOH + NaClO_2$) bleaching - Alkaline treatment - Grinding treatment	Cylindirical	35	–	–	–	[90]
Dunchi fiber	- Alkaline treatment - (H_2O_2+tetra-acetylethylenediamine, TAED) bleaching - ($CH_3COOH + HNO_3$) bleaching - Acid hydrolysis	Needles	20.67 ± 7.39	–	66.7	360	[91]
Palm wastes	- Alkaline treatment - Acid hydrolysis	Sphericles	42–82	–	27	–	[92]
Sugar palm fiber	- ILs pretreatment - H_2O_2 bleaching - WDM treatment	Thread-like structure	3.30 ± 0.68	96.89	61.62	360.5	Current study

homogenization (HPH), respectively. These yield discrepancies can be associated with factors including the material's source, pre-treatment processes, the number of processing cycles, and the temperature used in the mechanical approaches [97].

4.4. Surface properties of SPNFC

The surface area, pore size distribution, and pore volume characteristics of SPNFC were evaluated using nitrogen and Barrett-Joyner-Halenda (BJH) adsorption-desorption isotherms, as determined by BET analyses. The surface area of SPNFC is 3.46 m^2/g, highlighting its potential as a material with a large interface for improved performance. Balasubramani et al. [15] reported the high 7.3 m^2/g surface area of cellulose microfibrils (CMFs) from palmyra fruit peduncle waste. This feature presents advantages such as heightened adhesion, enhanced surface functionalization, and superior dispersion quality in polymer matrices. The determined pore volume (0.0057 cm^3/g) demonstrates SPNFC's capability for absorbing fluids and diffusion. Furthermore, with an average pore size of 4.47 nm, SPNFC is an excellent material for applications requiring reliable filtration. This feature might be attributed to the WDM treatment, resulting in an enhanced specific surface area owing to the decrease in average fiber diameter as proven by the TEM study.

A standard method for determining the surface charge of micro/nanomaterials, based on the basic concepts of suspension stability,

is the evaluation of zeta potential using the Zetasizer Nano-ZSP instrument. Zeta potential measures the degree of relative repulsion among colloidal particles and employs this information to determine the stability of a colloidal suspension [98]. This dynamic light scattering technique measured the approximate size of SPNFC particles and shows that SPNFC displayed notably negative zeta potential values (mV), with an average measurement of −32.1. Previous studies have shown that a zeta potential greater than ±25 mV is sufficient to establish suspension stability [43], indicating a suitable amount of nanofiber dispersion [99]. According to Carone et al. [100] suspensions with zeta potentials between ±10 to ±30 are in their early phases of instability, whereas those with zeta potentials between ±30 to ±40 are significantly more stable.

The negative zeta potential indicates a strong repulsive force among SPNFC particles, contributing to the stability of the colloidal suspension. The surface charge densities of SPNFC with better zeta potential offer opportunities for surface modification and interactions through functionalization or the introduction of specific groups of SPNFC with various materials. This opens avenues for tailoring SPNFC's properties to meet the requirements of specific applications. Moreover, the negative surface charge enhances the stability of SPNFC dispersion, reducing the likelihood of particle aggregation. In practical terms, this stability facilitates consistent and uniform dispersion when integrating SPNFC into composite materials or formulations. As the zeta potential is large, it indicates that there is a strong repulsive force between the particles, which improves the stability of the suspended and makes it less probable to flocculate [101]. In the context of potential interactions with other materials, the negative charge on SPNFC surfaces may influence its compatibility with positively charged components. This could be advantageous in applications such as composite materials, where the interaction between SPNFC and a polymer matrix is crucial for improving mechanical properties.

4.5. Crystallinity of SPNFC

The crystallinity of individual fibers was measured via XRD substantially influences the thermal and mechanical characteristics of the material [70]. The XRD diagrams of untreated SPF, SPF treated with ILs, SPC, and SPNFC are shown in Fig. 4. The peaks observed at $2\theta = 16^{\circ}$ and 22° in all diffractograms correspond to the distinctive cellulose I structure, as indicated by the XRD patterns. Table 3 shows the crystallinity index (Crl) determined on each sample. A notable increase in crystallinity is observed from raw SPF to IL-treated SPF and SPC, with Crl values rising from 50.97% to 52.69% and 67.18%, respectively. This enhancement is due to the removal of amorphous components that consist of lignin and hemicellulose according to the treatments used. The results align with previous research that showed that bleaching treatments increase crystallinity by removing lignin [102–104]. The CrI values for SPF after bleaching were higher than those for pomelo fruitlets (44.26%) and rice straw fibers (62.4%), as reported by He et al. [81] and Thakur et al. [105] correspondingly. Conversely, the implementation of WDM resulted in a reduction of crystallinity around 61.62%. Mechanical stresses caused by significant shear and friction via WDM can break down the crystalline structure of CNF, affecting a decrease in Crl values [41]. Studies on WDM treatment by Yasim-Anuar et al. [41] and Zakaria et al. [106] indicated similar findings.

4.6. Thermal stability of SPNFC

The study of the thermal behavior of the isolated compounds featured the utilization of a thermogravimetric analyzer for observing changes in weight as the temperature varied. The TGA and DTG curves of SPF following different treatments are shown in Fig. 5. The first weight loss of SPF, which occurs largely between 25 and 150 C, has been associated with the vaporization of volatile substances (water) within the samples [107]. Following that, in the second stage, significant weight losses were seen for all samples throughout the 200–360 °C range, consistent with cellulose and hemicellulose decomposition [108]. Nevertheless, different chemical components of untreated SPF, like hemicellulose, lignin, and cellulose, break down at different temperatures, leading to a degradation process with

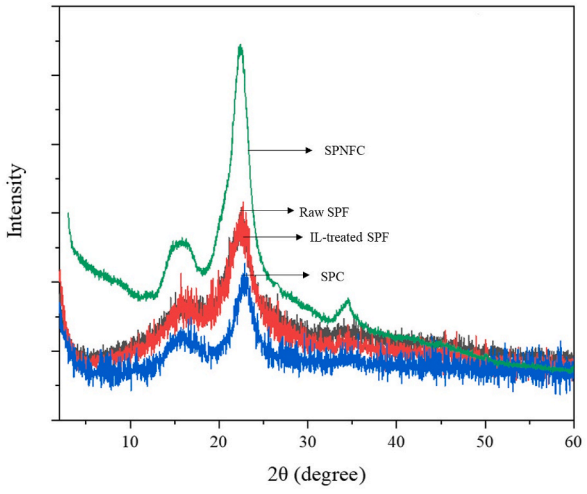

Fig. 4. XRD patterns of SPF at different treatment.

Table 3
X-ray crystallographic parameters for the synthesized samples.

Sample	2θ (am) (°)	2θ (200) (°)	CrI (%)
Raw SPF	19.38	22.48	50.97
ILs-treated SPF	19.18	22.74	52.69
SPC	19.10	22.90	67.18
SPNFC	18.14	22.42	61.62

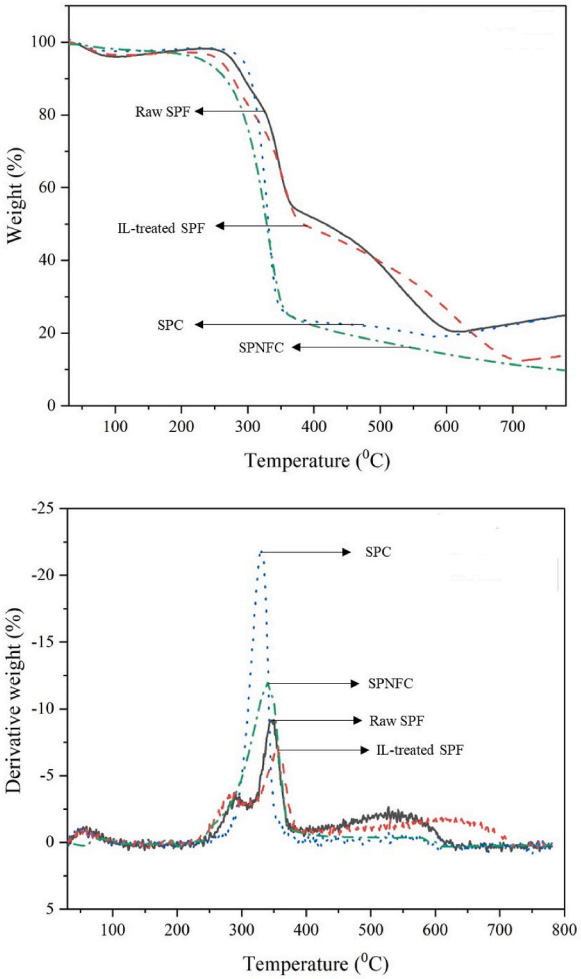

Fig. 5. TGA and DTG curves of SPF at different treatments.

multiple stages. Hemicellulose and cellulose degrade at 200–350 °C, followed by lignin decomposition at 350–480 °C, and the formation of char during lignin degradation more than 480 °C during this phase [109]. The raw SPF had a residual char of 25.6 wt% at 800 °C, which was higher than the treated SPF.

The DTG curve revealed distinct tri-peaks for both raw SPF and IL-treated SPF, contrasting with the dual peaks observed in SPC and SPNFC. The removal of lignin through the bleaching process leaves the fiber composition predominantly comprising hemicellulose and cellulose [96]. Hence, the WDM treatment facilitated the degradation process, given that hemicelluloses tend to degrade at lower temperatures (around 200–320 °C) compared to other macromolecular components like cellulose and lignin. According to the DTG curve, SPC has the largest peak, followed by SPNFC, Raw SPF, and then SPF treated with IL. As reported to Sayed et al. [109], the highest peak in the (DTG) profiles represents the point of most significant weight loss, and the height of this peak determines the reactivity of material from biomass.

5. Conclusions

This study has successfully extracted cellulose fibers from sugar palm fiber (SPF) using an eco-friendly ionic liquid (IL) pre-treatment followed by hydrogen peroxide bleaching treatments. Additionally, the study shows that the wet disk mill (WDM) method is effective and sustainable for extracting nano-fibrillated cellulose (NFC) from sugar palm cellulose, which results in a remarkable transformation of sugar palm fiber from a micro-scale to a mere 3 nm dimension as supported by the surface morphology study. Notably, the SPNFC has a negative zeta potential with absolute values greater than 30 mV, indicating good stability that successfully inhibits nanocellulose aggregation. This feature encourages the development of a strong network of nanofibers within polymer composite matrices. Significantly, XRD analysis disclosed an escalating trend in crystallinity for the treated SPF, advancing from 50.97% in raw SPFs to 52.69% in IL-treated fibers, surging to a peak of 67.18% in bleached SPF, and then declining to 61.62% with WDM treatments. This study highlights the vast potential of cellulose nanofiber, derived from sugar palm fiber, as a versatile material. Its remarkable surface properties, pore characteristics, surface charge densities, crystallinity, and thermal stability make it suitable for applications in advanced materials, biomedicine, and environmental engineering. The scalable and efficient extraction process further enhances the prospects of SPNFC as a sustainable and innovative material for various industries.

Availability of data and materials

The data supporting the findings of this study are available from the corresponding author upon request.

CRediT authorship contribution statement

A.S. Norfarhana: Writing – original draft, Resources, Methodology. **R.A. Ilyas:** Writing – review & editing, Supervision, Resources, Project administration. **Norzita Ngadi:** Writing – review & editing, Supervision. **Mohd Hafiz Dzarfan Othman:** Writing – review & editing, Supervision, Investigation.

Declaration of competing interest

The authors declare that they have no known competing financial interests or personal relationships that could have appeared to influence the work reported in this paper.

Acknowledgements

This project was funded by Universiti Teknologi Malaysia for the research project named “The impact of Malaysian bamboos’ chemical and fiber characteristics on their pulp and paper properties,” with grant number PY/2022/02318-Q.J130000.3851.21H99. The study was conducted as part of the Research Excellence Consortium program (JPT (BPKI) 1000/016/018/25 (57)), which is administered by the Ministry of Higher Education Malaysia (MOHE).

References

[1] A.A. Ghazali, S.A. Rahman, R.A. Samah, Potential of adsorbents from agricultural wastes as alternative fillers in mixed matrix membrane for gas separation: a review, Green Process. Synth. 9 (2020) 219–229, https://doi.org/10.1515/gps-2020-0023.
[2] M.J. Suriani, H.Z. Rapi, R.A. Ilyas, M. Petrů, S.M. Sapuan, Delamination and manufacturing defects in natural fiber-reinforced hybrid composite: a review, Polymers 13 (Apr. 2021) 1323, https://doi.org/10.3390/polym13081323.
[3] A.H. Alias, et al., Hybridization of MMT/lignocellulosic fiber reinforced polymer nanocomposites for structural applications: a review, Coatings 11 (2021) 1355, https://doi.org/10.3390/coatings11111355.
[4] V. Sharma, et al., Agro-industrial food waste as a low-cost substrate for sustainable production of industrial enzymes: a critical review, Catalysts 12 (2022) 1373, https://doi.org/10.3390/catal12111373.
[5] H. Mohamed, A.M. Shah, Y. Song, Conversion of agro-industrial wastes into value-added products, ACS Symp. Ser. 1392 (2021) 197–217, https://doi.org/10.1021/bk-2021-1392.ch010.
[6] U. Chadha, et al., A review of the function of using carbon nanomaterials in membrane filtration for contaminant removal from wastewater, Mater. Res. Express 9 (2022) 012003, https://doi.org/10.1088/2053-1591/ac48b8.
[7] B. Debnath, D. Haldar, M.K. Purkait, A critical review on the techniques used for the synthesis and applications of crystalline cellulose derived from agricultural wastes and forest residues, Carbohydr. Polym. 273 (2021) 118537, https://doi.org/10.1016/j.carbpol.2021.118537.
[8] H. Seddiqi, et al., Cellulose and its derivatives: towards biomedical applications, Springer Netherlands 28 (4) (2021), https://doi.org/10.1007/s10570-020-03674-w.
[9] M.M. Devarajan, G. Kumaraguruparan, K.J. Nagarajan, C. Vignesh, Production of hybrid AgNPs - TEMPO-mediated oxidation cellulose composite from jackfruit peduncle agro-waste and its thermal management application in electronic devices, Int. J. Biol. Macromol. 254 (2024) 127848, https://doi.org/10.1016/j.ijbiomac.2023.127848.
[10] F. Fahma, I. Febiyanti, N. Lisdayana, I.W. Arnata, D. Sartika, Nanocellulose as a new sustainable material for various applications: a review, Arch. Mater. Sci. Eng. 109 (2) (2021) 49–64, https://doi.org/10.5604/01.3001.0015.2624.
[11] S. Mbakop, L.N. Nthunya, M.S. Onyango, Recent advances in the synthesis of nanocellulose functionalized-hybrid membranes and application in water quality improvement, Processes 9 (2021) 611, https://doi.org/10.3390/pr9040611.
[12] A.S. Norfarhana, R.A. Ilyas, N. Ngadi, A review of nanocellulose adsorptive membrane as multifunctional wastewater treatment, Carbohydr. Polym. 291 (Sep. 2022) 119563, https://doi.org/10.1016/j.carbpol.2022.119563.
[13] A. Kadier, et al., Use of industrial wastes as sustainable nutrient sources for bacterial cellulose (BC) production: mechanism, advances, and future perspectives, Polymers 13 (2021) 3365, https://doi.org/10.3390/polym13193365.

[14] H. Abral, et al., Antimicrobial edible film prepared from bacterial cellulose nanofibers/starch/chitosan for a food packaging alternative, Int. J. Polym. Sci. 2021 (2021) 6641284, https://doi.org/10.1155/2021/6641284.

[15] S.T.K. Rajan, et al., Investigation of mechanical and thermo-mechanical characteristics of silane-treated cellulose nanofibers from agricultural waste reinforced epoxy adhesive composites, Int. J. Adhes. Adhes. 126 (2023) 103492, https://doi.org/10.1016/j.ijadhadh.2023.103492.

[16] G.R. Raghav, K.J. Nagarajan, M. Palaninatharaja, M. Karthic, R.A. Kumar, M.A. Ganesh, Reuse of used paper egg carton boxes as a source to produce hybrid AgNPs- carboxyl nanocellulose through bio-synthesis and its application in active food packaging, Int. J. Biol. Macromol. 249 (2023) 126119, https://doi.org/10.1016/j.ijbiomac.2023.126119.

[17] R.F. Dórame-Miranda, N. Gámez-Meza, L. Medina-Juárez, J.M. Ezquerra-Brauer, M. Ovando-Martínez, J. Lizardi-Mendoza, Bacterial cellulose production by Gluconacetobacter entanii using pecan nutshell as carbon source and its chemical functionalization, Carbohydr. Polym. 207 (August 2018) 91–99, https://doi.org/10.1016/j.carbpol.2018.11.067, 2019.

[18] D. Trache, et al., Nanocellulose: from Fundamentals to Advanced Applications, vol. 8, May. 2020, https://doi.org/10.3389/fchem.2020.00392.

[19] T.C. Mokhena, E.R. Sadiku, M.J. Mochane, S.S. Ray, M.J. John, A. Mtibe, Mechanical properties of cellulose nanofibril papers and their bionanocomposites: a review, Carbohydr. Polym. 273 (2021) 118507, https://doi.org/10.1016/j.carbpol.2021.118507.

[20] A.P.C. Almeida, J. Oliveira, S.N. Fernandes, M.H. Godinho, J.P. Canejo, All-cellulose composite membranes for oil microdroplet collection, Cellulose 27 (2020) 4665–4677, https://doi.org/10.1007/s10570-020-03077-x.

[21] R.S. Abolore, S. Jaiswal, A.K. Jaiswal, Green and sustainable pretreatment methods for cellulose extraction from lignocellulosic biomass and its applications: a review, Carbohydr. Polym. Technol. Appl. 7 (2024) 100396, https://doi.org/10.1016/j.carpta.2023.100396.

[22] S.S. Mohtar, T.N.Z. Tengku Malim Busu, A.M. Md Noor, N. Shaari, H. Mat, An ionic liquid treatment and fractionation of cellulose, hemicellulose and lignin from oil palm empty fruit bunch, Carbohydr. Polym. 166 (2017) 291–299, https://doi.org/10.1016/j.carbpol.2017.02.102 [Online]. Available:.

[23] S. Taokaew, W. Kriangkrai, Recent progress in processing cellulose using ionic liquids as solvents, Polysaccharides 3 (2022) 671–691, https://doi.org/10.3390/polysaccharides3040039.

[24] A.S. Norfarhana, R.A. Ilyas, N. Ngadi, M.H.D. Othman, M.S.M. Misenan, M.N.F. Norrrahim, Revolutionizing lignocellulosic biomass: a review of harnessing the power of ionic liquids for sustainable utilization and extraction, Int. J. Biol. Macromol. 256 (2024) 128256, https://doi.org/10.1016/j.ijbiomac.2023.128256.

[25] C.M. Patil, A.U. Borse, J.S. Meshram, Ionic liquid: green solvent for the synthesis of cellulose/guar gum/PVA biocomposite, Green Mater. 6 (1) (2018) 23–29.

[26] R. Financie, M. Moniruzzaman, Y. Uemura, Enhanced enzymatic delignification of oil palm biomass with ionic liquid pretreatment, Biochem. Eng. J. 110 (1–7) (2016), https://doi.org/10.1016/j.bej.2016.02.008 [Online]. Available:.

[27] M. Lara-Serrano, S. Morales-delaRosa, J.M. Campos-Martín, J.L.G. Fierro, Fractionation of lignocellulosic biomass by selective precipitation from ionic liquid dissolution, Appl. Sci. 9 (2019) 1862.

[28] M. Moniruzzaman, T. Ono, Separation and characterization of cellulose fibers from cypress wood treated with ionic liquid prior to laccase treatment, Bioresour. Technol. 127 (2013) 132–137, https://doi.org/10.1016/j.biortech.2012.09.113 [Online]. Available:.

[29] Z. Ullah, et al., Extraction of valuable chemicals from sustainable rice husk waste using ultrasonic assisted ionic liquids technology, J. Clean. Prod. 220 (2019) 620–629, https://doi.org/10.1016/j.jclepro.2019.02.041.

[30] W. Klunklin, S. Hinmo, P. Thipchai, P. Rachtanapun, Effect of bleaching processes on physicochemical and functional properties of cellulose and carboxymethyl cellulose from Young and mature coconut coir, Polymers 15 (2023) 3376, https://doi.org/10.3390/polym15163376.

[31] C.T.X. Nguyen, K.H. Bui, B.Y. Truong, N.H.N. Do, P.T.K. Le, Nanocellulose from pineapple leaf and its applications towards high-value engineering materials, Chem. Eng. Trans. 89 (2021) 19–24, https://doi.org/10.3303/CET2189004.

[32] Y. Wu, J. Wu, F. Yang, C. Tang, Q. Huang, Effect of H2O2 bleaching treatment on the properties of finished transparent wood, Polymers 11 (2019) 776, https://doi.org/10.3390/polym11050776.

[33] N.E. Fitriana, A. Suwanto, T.H. Jatmiko, S. Mursiti, D.J. Prasetyo, Cellulose extraction from sugar palm (Arenga pinnata) fibre by alkaline and peroxide treatments, IOP Conf. Ser. Earth Environ. Sci. 462 (1) (2020), https://doi.org/10.1088/1755-1315/462/1/012053.

[34] M.T. Garnett, H.K. Senthil Kumar, B.S. Beckingham, S.L.M. Alexander, Extraction of cellulose from restaurant food waste, RSC Sustain 2 (2024) 170–178, https://doi.org/10.1039/d3su00192j.

[35] M.M. Zainol, N.S.A. Rasid, M. Asmadi, N.A.S. Amin, Carboxymethyl cellulose synthesis from treated oil palm empty fruit bunch using ionic liquid and Hydrogen Peroxide, ASEAN Eng. J. 11 (4) (2021) 80–88, https://doi.org/10.11113/AEJ.V11.17866.

[36] M. Rizwan, S.R. Gilani, A.I. Durrani, S. Naseem, Cellulose extraction of Alstonia scholaris: a comparative study on efficiency of different bleaching reagents for its isolation and characterization, Int. J. Biol. Macromol. 191 (2021) 964–972, https://doi.org/10.1016/j.ijbiomac.2021.09.155.

[37] H. Kargarzadeh, M. Ioelovich, I. Ahmad, S. Thomas, A. Dufresne, Methods for extraction of nanocellulose from various sources, Handb. Nanocellulose Cellul. Nanocomposites (2017) 1–49, https://doi.org/10.1002/9783527689972.ch1.

[38] Y. Pei, L. Wang, K. Tang, D.L. Kaplan, Biopolymer nanoscale assemblies as building blocks for new materials: a review, Adv. Funct. Mater. 31 (2021) 2008552, https://doi.org/10.1002/adfm.202008552.

[39] A. Salama, et al., Nanocellulose-based materials for water treatment: adsorption, photocatalytic degradation, disinfection, antifouling, and nanofiltration, Nanomaterials 11 (2021) 3008, https://doi.org/10.3390/nano11113008.

[40] M.N.F. Norrrahim, et al., Greener pretreatment approaches for the valorisation of natural fibre biomass into bioproducts, Polymers 13 (2021) 2971, https://doi.org/10.3390/polym13172971.

[41] T.A.T. Yasim-Anuar, N.S. Sharip, L.N. Megashah, H. Ariffin, N.A.M. Nor, Cellulose nanofibers from waste paper and their utilization as reinforcement materials in poly((r)-3-hydroxybutyrate-co-(r)-3-hydroxyhexanoate bionanocomposite, Pertanika J. Sci. Technol. 28 (2020) 259–271, https://doi.org/10.47836/pjst.28.S2.20. Special issue 2.

[42] M. Imraan, R.A. Ilyas, A.S. Norfarhana, S.P. Bangar, V.F. Knight, M.N.F. Norrrahim, Sugar palm (Arenga pinnata) fibers: new emerging natural fibre and its relevant properties, treatments and potential applications, J. Mater. Res. Technol. 24 (2023) 4551–4572, https://doi.org/10.1016/j.jmrt.2023.04.056.

[43] R.A. Ilyas, S.M. Sapuan, M.R. Ishak, E.S. Zainudin, Sugar palm nanofibrillated cellulose (Arenga pinnata (Wurmb.) Merr): effect of cycles on their yield, physic-chemical, morphological and thermal behavior, Int. J. Biol. Macromol. 123 (2019) 379–388.

[44] M.R.M. Asyraf, et al., Recent advances of thermal properties of sugar palm lignocellulosic fibre reinforced polymer composites, Int. J. Biol. Macromol. 193 (2021) 1587–1599, https://doi.org/10.1016/j.ijbiomac.2021.10.221.

[45] S.F.K. Sherwani, E.S. Zainudin, S.M. Sapuan, Z. Leman, K. Abdan, Mechanical properties of sugar palm (Arenga pinnata wurmb. merr)/glass fiber-reinforced poly(lactic acid) hybrid composites for potential use in motorcycle components, Polymers 13 (2021) 3061, https://doi.org/10.3390/polym13183061.

[46] M.R.M. Asyraf, et al., Sugar palm fibre-reinforced polymer composites : influence of chemical treatments on its mechanical properties, Materials 15 (2022) 3852.

[47] A. Nazrin, S.M. Sapuan, M.Y.M. Zuhri, I.S.M.A. Tawakkal, R.A. Ilyas, Water barrier and mechanical properties of sugar palm crystalline nanocellulose reinforced thermoplastic sugar palm starch (TPS)/poly(lactic acid) (PLA) blend bionanocomposites, Nanotechnol. Rev. 10 (1) (2021) 431–442, https://doi.org/10.1515/ntrev-2021-0033.

[48] R.A. Ilyas, et al., Sugar palm (Arenga pinnata [Wurmb.] Merr) starch films containing sugar palm nanofibrillated cellulose as reinforcement: water barrier properties, Polym. Compos. (2019) 1, https://doi.org/10.1002/pc.25379. –9.

[49] R.A. Ilyas, et al., Effect of sugar palm nanofibrillated cellulose concentrations on morphological, mechanical and physical properties of biodegradable films based on agro-waste sugar palm (Arenga pinnata(Wurmb.) Merr) starch, J. Mater. Res. Technol. 8 (5) (2019), https://doi.org/10.1016/j.jmrt.2019.08.028.

[50] R.A. Ilyas, S.M. Sapuan, M.R. Ishak, E.S. Zainudin, Development and characterization of sugar palm nanocrystalline cellulose reinforced sugar palm starch bionanocomposites, Carbohydr. Polym. 202 (2018) 186–202, https://doi.org/10.1016/j.carbpol.2018.09.002.

[51] A. Nazrin, S.M. Sapuan, M.Y.M. Zuhri, Mechanical, physical and thermal properties of sugar palm nanocellulose reinforced thermoplastic starch (TPS)/Poly (Lactic Acid) (PLA) blend bionanocomposites, Polymers 12 (2020) 2216, https://doi.org/10.3390/polym12102216.

[52] I. Mukhtar, Z. Leman, M.R. Ishak, E.S. Zainudin, Sugar palm fibre and its composites: a review of recent developments, Bioresources 11 (4) (2016) 10756–10782, https://doi.org/10.15376/biores.11.4.10756-10782.
[53] A. Barhoum, et al., Nanocelluloses as sustainable membrane materials for separation and filtration technologies: principles, opportunities, and challenges, Carbohydr. Polym. 317 (2023) 121057, https://doi.org/10.1016/j.carbpol.2023.121057.
[54] A.S. Norfarhana, R.A. Ilyas, N. Ngadi, M.H.D. Othman, Optimization of ionic liquid pretreatment of sugar palm fiber for cellulose extraction, J. Mol. Liq. 398 (2024) 124256, https://doi.org/10.1016/j.molliq.2024.124256.
[55] S. Susi, M. Ainuri, W. Wagiman, M.A.F. Falah, Effect of delignification and bleaching stages on cellulose purity of oil palm empty fruit bunches, IOP Conf. Ser. Earth Environ. Sci. 1116 (2022) 012018, https://doi.org/10.1088/1755-1315/1116/1/012018.
[56] M.J. Khan, et al., Fabrication and characterization of functional biobased membranes from postconsumer cotton fabrics and palm waste for the removal of dyes, Int. J. Mol. Sci. 24 (2023) 6030, https://doi.org/10.3390/ijms24076030.
[57] P. Liu, C. Zhu, A.P. Mathew, Mechanically robust high flux graphene oxide - nanocellulose membranes for dye removal from water, J. Hazard Mater. 371 (2019) 484–493, https://doi.org/10.1016/j.jhazmat.2019.03.009.
[58] L. Segal, J.J. Creely, A.E. Martin, C.M. Conrad, An empirical method for estimating the degree of crystallinity of native cellulose using the X-ray diffractometer, Text. Res. J. 29 (1959) 786–794, https://doi.org/10.1177/004051755902901003.
[59] X. Han, et al., Micro- and nano-fibrils of manau rattan and solvent-exchange-induced high-haze transparent holocellulose nanofibril film, Carbohydr. Polym. 298 (2022) 120075, https://doi.org/10.1016/j.carbpol.2022.120075.
[60] A.D. French, Increment in evolution of cellulose crystallinity analysis, Cellulose 27 (2020) 5445–5448, https://doi.org/10.1007/s10570-020-03172-z.
[61] A.D. French, Idealized powder diffraction patterns for cellulose polymorphs, Cellulose 21 (2014) 885–896, https://doi.org/10.1007/s10570-013-0030-4.
[62] E. Amini, C. Valls, M.B. Roncero, Ionic liquid-assisted bioconversion of lignocellulosic biomass for the development of value-added products, J. Clean. Prod. 326 (2021) 129275, https://doi.org/10.1016/j.jclepro.2021.129275.
[63] B. Azimi, et al., Cellulose-based fiber spinning processes using ionic liquids, Cellulose 29 (2022) 3079–3129, https://doi.org/10.1007/s10570-022-04473-1.
[64] E. Pinto, et al., Cellulose processing from biomass and its derivatization into carboxymethylcellulose: a review, Sci. African 15 (2022) e01078, https://doi.org/10.1016/j.sciaf.2021.e01078.
[65] E. Syafri, Jamaluddin, N.H. Sari, M. Mahardika, P. Amanda, R.A. Ilyas, Isolation and characterization of cellulose nanofibers from Agave gigantea by chemical-mechanical treatment, Int. J. Biol. Macromol. 200 (2022) 25–33, https://doi.org/10.1016/j.ijbiomac.2021.12.111.
[66] K.O. Ejeta, T.O. Azeez, A.T. Banigo, K.I. Nkuma-Udah, E. Ajuogu, Isolation and characterization of cellulose nanofibres from three common Nigerian grasses, IOP Conf. Ser. Mater. Sci. Eng. 805 (2020) 012040, https://doi.org/10.1088/1757-899X/805/1/012040.
[67] C.K. Saurabh, et al., Isolation and characterization of cellulose nanofibers from gigantochloa scortechinii as a reinforcement material, J. Nanomater. (2016) 4024527, https://doi.org/10.1155/2016/4024527.
[68] M.A.F. Supian, K.N.M. Amin, S.S. Jamari, S. Mohamad, Production of cellulose nanofiber (CNF) from empty fruit bunch (EFB) via mechanical method, J. Environ. Chem. Eng. 8 (2020) 103024, https://doi.org/10.1016/j.jece.2019.103024.
[69] K.J. Nagarajan, et al., Extraction of cellulose nanocrystals from red banana peduncle agro-waste and application in environmentally friendly biocomposite film, Polym. Compos. 43 (2022) 4942–4958, https://doi.org/10.1002/pc.26755.
[70] R.A. Ilyas, S.M. Sapuan, M.R. Ishak, E.S. Zainudin, Effect of delignification on the physical, thermal, chemical, and structural properties of sugar palm fibre, Bioresources 12 (4) (2017) 8734–8754.
[71] J. Li, D. Liu, J. Li, F. Yang, G. Sui, Y. Dong, Fabrication and properties of tree-branched cellulose nanofibers (CNFs) via acid hydrolysis assisted with pre-disintegration treatment, Nanomaterials 12 (2022) 2089, https://doi.org/10.3390/nano12122089.
[72] M.R.K. Sofla, R.J. Brown, T. Tsuzuki, T.J. Rainey, A comparison of cellulose nanocrystals and cellulose nano fi bres extracted from bagasse using acid and ball milling methods, Adv. Nat. Sci. Nanosci. Nanotechnol. 7 (2016) 035004.
[73] N. Atykyan, V. Revin, V. Shutova, Raman and FT - IR Spectroscopy investigation the cellulose structural differences from bacteria Gluconacetobacter sucrofermentans during the different regimes of cultivation on a molasses media, Amb. Express 10 (84) (2020), https://doi.org/10.1186/s13568-020-01020-8.
[74] V. Hospodarova, E. Singovszka, N. Stevulova, Characterization of cellulosic fibers by FTIR spectroscopy for their further implementation to building materials, Am. J. Anal. Chem. 9 (2018) 303–310, https://doi.org/10.4236/ajac.2018.96023.
[75] R.A. Ilyas, S.M. Sapuan, M.R. Ishak, Isolation and characterization of nanocrystalline cellulose from sugar palm fibres (Arenga Pinnata), Carbohydr. Polym. 181 (2018) 1038–1051.
[76] M.S. Cintrón, D.J. Hinchliffe, FT-IR examination of the development of secondary cell wall in cotton fibers, Fibers 3 (2015) 30–40, https://doi.org/10.3390/fib3010030.
[77] V. Suthar, A. Pratap, H. Raval, Studies on poly (hydroxy alkanoates)/(ethylcellulose) blends, Bull. Mater. Sci. 23 (3) (2000) 215–219.
[78] H. Wang, J. Wu, Y. Lian, Y. Li, B. Huang, Q. Lu, Zirconium phosphate assisted phosphoric acid Co-catalyzed hydrolysis of lignocellulose for enhanced extraction of nanocellulose, Polymers 15 (2023) 447, https://doi.org/10.3390/polym15020447.
[79] P.R.L. Lima, H.M. Santos, G.P. Camilloto, R.S. Cruz, Effect of surface biopolymeric treatment on sisal fiber properties and fiber-cement bond, J. Eng. Fiber. Fabr. 12 (2) (2017) 59–71, https://doi.org/10.1177/155892501701200207.
[80] L. Jiang, et al., Preparation and characterization of porous cellulose acetate nanofiber hydrogels, Gels 9 (2023) 484, https://doi.org/10.3390/gels9060484.
[81] C. He, H. Li, J. Hong, H. Xiong, H. Ni, M. Zheng, Characterization and functionality of cellulose from pomelo fruitlets by different extraction methods, Polymers 14 (2022) 518.
[82] T. Hong, J. Yin, S. Nie, M. Xie, Applications of infrared spectroscopy in polysaccharide structural analysis : progress , challenge and perspective, Food Chem. X 12 (2021) 100168, https://doi.org/10.1016/j.fochx.2021.100168.
[83] C.D. Midhun Dominic, et al., Chlorine-free extraction and structural characterization of cellulose nanofibers from waste husk of millet (Pennisetum glaucum), Int. J. Biol. Macromol. 206 (2022) 92–104, https://doi.org/10.1016/j.ijbiomac.2022.02.078.
[84] C.D. Midhun Dominic, et al., Cellulose nanofibers isolated from the Cuscuta Reflexa plant as a green reinforcement of natural rubber, Polymers 12 (2020) 814, https://doi.org/10.3390/POLYM12040814.
[85] B.K. Mahur, A. Ahuja, S. Singh, P.K. Maji, V.K. Rastogi, Different nanocellulose morphologies (cellulose nanofibers, nanocrystals and nanospheres) extracted from Sunn hemp (Crotalaria Juncea), Int. J. Biol. Macromol. 253 (2023) 126657, https://doi.org/10.1016/j.ijbiomac.2023.126657.
[86] E. Syafri, Jamaluddin, N.H. Sari, M. Mahardika, P. Amanda, R.A. Ilyas, Isolation and characterization of cellulose nanofibers from Agave gigantea by chemical-mechanical treatment, Int. J. Biol. Macromol. 200 (2022) 25–33, https://doi.org/10.1016/j.ijbiomac.2021.12.111.
[87] R.K. Gond, M.K. Gupta, M. Jawaid, Extraction of nanocellulose from sugarcane bagasse and its characterization for potential applications, Polym. Compos. 42 (2021) 5400–5412, https://doi.org/10.1002/pc.26232.
[88] N. Samsalee, J. Meerasri, R. Sothornvit, Rice husk nanocellulose: extraction by high-pressure homogenization, chemical treatments and characterization, Carbohydr. Polym. Technol. Appl. 6 (2023) 100353, https://doi.org/10.1016/j.carpta.2023.100353.
[89] K. Diharjo, F. Gapsari, A. Andoko, R. Septiari, S.M. Rangappa, S. Siengchin, Optimization of nano cellulose extraction from timoho fiber using response surface methodology (RSM), Biomass Convers. Biorefinery (2023), https://doi.org/10.1007/s13399-023-04551-9.
[90] A. Kumar Trivedi, A. Kumar, M.K. Gupta, Extraction of nanocellulose from wheat straw and its characterization, Mater. Today Proc. 78 (2022) 48–54, https://doi.org/10.1016/j.matpr.2022.11.038.
[91] M.N. Khan, N. Rehman, A. Sharif, E. Ahmed, Z.H. Farooqi, M.I. Din, Environmentally benign extraction of cellulose from dunchi fiber for nanocellulose fabrication, Int. J. Biol. Macromol. 153 (2020) 72–78, https://doi.org/10.1016/j.ijbiomac.2020.02.333.
[92] S. Mehanny, et al., Extraction and characterization of nanocellulose from three types of palm residues, J. Mater. Res. Technol. 10 (2021) 526–537, https://doi.org/10.1016/j.jmrt.2020.12.027.
[93] A. Kumagai, et al., Improvement of enzymatic saccharification of Populus and switchgrass by combined pretreatment with steam and wetdiskmilling, Renew. Energy 76 (2015) 782–789, https://doi.org/10.1016/j.renene.2014.11.070.

[94] N. Masruchin, P. Amanda, W.B. Kusumaningrum, L. Suryanegara, A. Nuryawan, Particle size distribution and yield analysis of different charged cellulose nanofibrils obtained by TEMPO-mediated oxidation, IOP Conf. Ser. Earth Environ. Sci. 572 (2020) 012045, https://doi.org/10.1088/1755-1315/572/1/012045.
[95] S. Jonasson, A. Bünder, T. Niittylä, K. Oksman, Isolation and characterization of cellulose nanofibers from aspen wood using derivatizing and non-derivatizing pretreatments, Cellulose 27 (2020) 185–203, https://doi.org/10.1007/s10570-019-02754-w.
[96] R.A. Ilyas, S.M. Sapuan, M.R. Ishak, Isolation and characterization of nanocrystalline cellulose from sugar palm fibres (Arenga Pinnata), Carbohydr. Polym. 181 (2018) 1038–1051, https://doi.org/10.1016/j.carbpol.2017.11.045.
[97] H.P.S. Abdul Khalil, et al., Production and modification of nanofibrillated cellulose using various mechanical processes: a review, Carbohydr. Polym. 99 (2014) 649–665, https://doi.org/10.1016/j.carbpol.2013.08.069.
[98] M. Kosmulski, M. Kalbarczyk, Zeta potential of nanosilica in 50% aqueous ethylene glycol and in 50% aqueous propylene glycol, Molecules 28 (2023) 1335, https://doi.org/10.3390/molecules28031335.
[99] A. Sharma, T. Mandal, S. Goswami, Dispersibility and stability studies of cellulose nanofibers: implications for nanocomposite preparation, J. Polym. Environ. 29 (5) (2021) 1516–1525, https://doi.org/10.1007/s10924-020-01974-7.
[100] A. Carone, S. Emilsson, P. Mariani, A. Désert, S. Parola, Gold nanoparticle shape dependence of colloidal stability domains, Nanoscale Adv. 5 (7) (2023) 2017–2026, https://doi.org/10.1039/D2NA00809B.
[101] F. Whba, F. Mohamed, M.I. Idris, M.S. Yahya, Surface modification of cellulose nanocrystals (CNCs) to form a biocompatible, stable, and hydrophilic substrate for MRI, Appl. Sci. 13 (2023) 6316, https://doi.org/10.3390/app13106316.
[102] A.S. Hozman-Manrique, A.J. Garcia-Brand, M. Hernández-Carrión, A. Porras, Isolation and characterization of cellulose microfibers from Colombian cocoa pod husk via chemical treatment with pressure effects, Polymers 15 (2023) 664, https://doi.org/10.3390/polym15030664.
[103] L.A. Worku, R.K. Bachheti, M.G. Tadesse, Isolation and characterization of natural cellulose from oxytenanthera abyssinica (lowland Ethiopian bamboo) using alkali peroxide bleaching stages followed by aqueous chlorite in buffer solution, Int. J. Polym. Sci. 2022 (2022), https://doi.org/10.1155/2022/5155552.
[104] H. Amirulhakim, A.L. Juwono, S. Roseno, Isolation and characterization of cellulose nanofiber from subang pineapple leaf fiber waste produced using ultrafine grinding method, IOP Conf. Ser. Mater. Sci. Eng. 1098 (2021) 062067, https://doi.org/10.1088/1757-899x/1098/6/062067.
[105] M. Thakur, A. Sharma, V. Ahlawat, M. Bhattacharya, S. Goswami, Process optimization for the production of cellulose nanocrystals from rice straw derived α-cellulose, Mater. Sci. Energy Technol. 3 (2020) 328–334, https://doi.org/10.1016/j.mset.2019.12.005.
[106] M.R. Zakaria, M.N.F. Norrrahim, S. Hirata, M.A. Hassan, Hydrothermal and wet disk milling pretreatment for high conversion of biosugars from oil palm mesocarp fiber, Bioresour. Technol. 181 (2015) 263–269, https://doi.org/10.1016/j.biortech.2015.01.072.
[107] S. Cichosz, A. Masek, Cellulose fibers hydrophobization via a hybrid chemical modification, Polymers 11 (2019) 1174, https://doi.org/10.3390/polym11071174.
[108] J. Wang, E. Minami, M. Asmadi, H. Kawamoto, Effect of delignification on thermal degradation reactivities of hemicellulose and cellulose in wood cell walls, J. Wood Sci. 67 (19) (2021), https://doi.org/10.1186/s10086-021-01952-0.
[109] S.A. El-Sayed, T.M. Khass, M.E. Mostafa, Thermal degradation behaviour and chemical kinetic characteristics of biomass pyrolysis using TG/DTG/DTA techniques, Biomass Convers. Biorefinery (2023), https://doi.org/10.1007/s13399-023-03926-2.